Double Plane Wave Kirchhoff Depth Migration

P.L. Stoffa*, M.K. Sen, and R.K. Seifoullaev, Institute for Geophysics, The University of Texas at Austin,
R. Pestana, Universidade Federal da Bahia, Brazil, J.T. Fokkema, TU Delft, The Netherlands

Abstract

We present a migration method in the coupled ray-parameter domain that is fast and efficient for seismic data that are densely sampled in the source-receiver configuration space. The method is based on slant stacking over both shot positions and receiver positions (or offsets) for all the recorded data. If the data acquisition geometry permits, both in-line and cross-line source positions and receiver positions (or offsets) can be incorporated into a multidimensional phase velocity space which is regular even for randomly positioned input data. By noting the maximum time dips that are present in the shot and receiver gathers and constant offset sections, the number of plane waves required can be estimated and this generally results in a data reduction of at least one and possibly two orders of magnitude. The required travel time computations for depth imaging are independent for each particular plane wave component and thus can be used for either the source or the receiver plane waves during extrapolation in phase space, reducing considerably the computational burden. Even so, each source and receiver plane wave component must be combined with all other receiver and source components for a complete diffraction summation. Since only vertical delay times are required, many travel time techniques can be employed and the problems with multi-pathing and first arrivals are either reduced or eliminated. Further, the shot plane wave integral can be pruned to concentrate the image on selected targets. In this way the computation time can be further reduced and the technique lends itself naturally to a velocity modeling scheme where for example, horizontal and then steeply dipping events are gradually introduced into the analysis. Of course this imaging scheme can be implemented in parallel using a distributed architecture like a PC cluster to compute various plane wave sections since they are independent of each other. The common ray-parameter image gathers can be used exactly like common angle image gathers for residual migration velocity analysis. The migration method lends itself to imaging in anisotropic media since phase space is the natural domain for such an analysis.

Introduction

Typically the $\tau - p$ transformation is performed for each recorded seismic trace relative to its fixed source position (that is, with respect to the receiver's offset relative to the source position, see Schultz and Claerbout, 1978; Stoffa et al., 1981). Given modern multi-coverage data $P(s,r,t)$, where s is the source location and r is the receiver location, there is no practical reason or obstacle not to apply the $\tau - p$ transformation with respect to r, or s, or even both (Fokkema and van den Berg, 1993).

In the frequency domain the decomposition of the recorded data $P(s,r,t)$ into source and receiver plane-wave components is accomplished using a variant of slant stacking which uses a linear phase delay of each trace with respect to its shot or receiver position. For receiver plane waves, we have the following forward and inverse stacking formulas:

$$P(s,p_r,\omega) = \int P(s,r,\omega)\exp(+i\omega p_r r)dr,$$
$$P(s,r,\omega) = \omega^2 \int P(s,p_r,\omega)\exp(-i\omega p_r r)dp_r,$$

where ω is angular frequency, $P(s,p_r,\omega)$ represents the plane-wave data with ray parameter p_r with respect to the absolute source and receiver positions.

The above variant of slant stacking can be applied to decompose all recorded source and receiver data simultaneously into plane waves using

$$P(p_s,p_r,\omega) = \iint P(s,r,\omega)\exp(+i\omega[p_s s + p_r r])dsdr, \qquad (1)$$

with the inverse slant-stack given by

$$P(s,r,\omega) = \omega^4 \iint P(p_s,p_r,\omega)\exp(-i\omega[p_s s + p_r r])dp_s dp_r, \qquad (2)$$

Kirchhoff integral

In the frequency domain the Kirchhoff integral (Stolt, 1978; Schneider, 1978) for wavefield continuation of sources and receivers to depth is

$$P(x,\omega) = \int \partial_n G(x,s,\omega)ds \int \partial_n G(x,r,\omega)P(s,r,\omega)dr\ , \qquad (3)$$

where $P(s,r,\omega)$ is the seismic wavefield measured at the surface, G is the Green's function, $\partial_n G$ is the surface normal derivative of the Green's function, x is the subsurface location, and $P(x,\omega)$ is the predicted wavefield at depth. To extrapolate the measured seismic wavefield $P(s,r,\omega)$ we need to construct the Green's function. For heterogeneous medium the Green's function is approximated using asymptotic ray theory (ART). In this way the Green's function is represented by a high-frequency approximation given by

$$G(x,s,\omega) = A(x,s)\exp(i\omega t(x,s))\ ,$$

where $A(x,\ s)$ is an amplitude term and $t(x,s)$ is the ray travel time from the source s to the image point x.

Using the ART approximation and making the assumption that the amplitude is a slowly varying function of space (Hildebrand and Carrol, 1993) equation (3) can be rewritten as

$$P(x,\omega) = -\omega^2 W(x)\int P(s,r,\omega)ds \int \exp(i\omega[t(x,s)+t(x,r)])dr, \quad (4)$$

where $W(x) = \partial_n t(x,s)A(x,s)\partial_n t(x,r)A(x,r)$.

Transforming simultaneously all shot and receiver gathers to plane waves according to equation (2) and defining the receiver and source vertical delay times respectively as

$\tau(x,s,p_s) = t(x,s) - p_s s$,

$\tau(x,r,p_r) = t(x,r) - p_r r$,

we get for the plane wave (p_s, p_r):

$$P(x,p_s,p_r,\omega) = -\omega^6 W(x)P(p_s,p_r,\omega)\cdot \iint \exp(i\omega[\tau(x,s,p_s)+\tau(x,r,p_r)])dsdr. \quad (5)$$

Summing over all frequencies and all plane wave combinations forms the final image:

$$P(x) = -W(x)\iiint \omega^6 P(p_s,p_r,\omega)d\omega dp_s dp_r \iint \exp(i\omega[\tau(x,s,p_s)+\tau(x,r,p_r)])dsdr. \quad (6)$$

Denoting by ξ the projection of x onto the measurement surface we note that

$$\tau(x,s,p_s) = \tau(x,p_s) - p_s\xi, \quad \tau(x,r,p_r) = \tau(x,p_r) - p_r\xi, \quad (7)$$

where $\tau(x,p_s),\tau(x,p_r)$ are the source and receiver vertical delay times computed from the origin to the isochron of x, respectively (see Figure 1). Substituting equations (7) into (6) and after some simplification we obtain

$$P(x) = -K(x)\iiint P(p_s,p_r,\omega) \exp(i\omega[\tau(x,p_s)+\tau(x,p_r)+(p_s+p_r)\xi)])d\omega dp_s dp_r, \quad (8)$$

where $K(x)$ differs from $W(x)$ only by a contstant factor. Noting that integral over frequencies represents δ function, we finally arrive at the double plane wave Kirchhoff imaging formula:

$$P(x) = -K(x)\iint P(p_s,p_r,\tau(x,p_s)+\tau(x,p_r)+(p_s+p_r)\xi)dp_s dp_r \text{ ,} \quad (9)$$

Equation (9) can be rewritten in source-offset coordinates. If we change variables $o = r - s$, $s' = s$, then according to the chain rule $p_r = p_o, p_s = p_{s'} - p_o$. Assuming field invariance under the change of variables and dropping the primes equation (9) becomes

$$P(x) = -K(x)\iint P(p_s,p_o,\tau(x,p_s-p_o)+\tau(x,p_o)+p_s\xi)dp_s dp_o \text{ .} \quad (10)$$

Discussion

Kirchhoff plane wave migration has several advantages over conventional offset domain migrations methods. First, the plane wave transforms regularize the observational data as part of a pre-imaging process. Second, plane wave data are sparser than the recorded data so smaller data volumes are used in the imaging algorithm. Also, relevant subsets or plane wave components can be used for target illumination and velocity analysis studies.

The main advantage, however, comes from the realization that because of Figure 1 and equations (7), the vertical delay times that need to be computed are independent of the source and receiver positions except for a simple horizontal delay time correction. In addition, many of the same vertical delay times are required for imaging either source, receiver or offset plane waves and need be calculated only once.

Finally, since the plane wave domain is the equivalent of a phase velocity representation, anisotropy can be taken into account exactly, using for example the delay time computation methods described by Mukherjee et. al. (2005).

Examples

The examples are based on a 2D staggered grid elastic finite difference simulation, (Levander, 1988) for the EAEG salt data, see Figure 2. The data were acquired every 20m along the top of the model for 675 shot positions. The acquisition proceeded from the left (X=0.0km) to the right (X=13.48 km). We simulated a marine survey with a receiver array towed behind the ship. 240 channels were acquired with the first complete shot gather occurring at shot point 240 (X=4.78 km). The receiver spacing was 20 m. The first layer was water and only pressure was recorded. Absorbing boundaries were added to the model to limit reflections from the edges and bottom of the model and to minimize surface related multiples. For example shot records from the middle of the survey and over the salt are shown in Figure 3.

Results

The original shot gather data were transformed into the conventional offset plane wave domain by simple slant stacking. 121 plane wave seismograms for ray parameters +0.6 to -0.6 sec/km every 0.01 sec/km were recovered from the input shot gathers. The origin was taken relative to each shot's position and the plane wave gathers of Figure 4 correspond to the common shot gathers of Figure 3.

The original data were also simultaneously transformed to construct both source and receiver plane waves using equation (1). This process completely transforms the data into plane wave components. The appearance of this reduced data volume is not easy to interpret so we show several cuts through the volume in Figure 5, for all p_r plane waves for the cases where p_s = -0.5, p_s = 0.0 and p_s = 0.5 sec/km from left to right in three panels.

We also transformed the data to source and offset plane waves. Figure 6 shows the case for all p_o plane waves for the cases where p_s = -0.5, p_s = 0.0 and p_s = 0.5 sec/km from left to right in three panels. Here the p_s = 0.0 (center) gather corresponding to horizontal reflectors dominates the others and appears similar to a conventional single shot $\tau - p_o$ gather. Figure 7 shows the opposite case, for p_o =0.0 sec/km and all source plane waves.

The p_s–p_o volume was migrated using equation (10) and an eikonal solver, see Schneider et al., 1992, to calculate the vertical delay times. Each constant offset ray parameter plane wave section was migrated independently of the others and in parallel. Once all plane wave sections were migrated, the resulting common image gathers were stacked to generate the final image.

Plane wave vertical delay times were reused once computed as appropriate. For example, vertical delay times for any p, whether p_r, p_o or p_s, can be reused whether we need a p_s, p_r or a p_o as long as it has previously been computed.

Figure 8 shows the result for a targeted imaging where we used all 121 p_o plane waves but limit the p_s aperture to -0.1 to +0.1 sec/km about each p_o plane wave being imaged. This means that we are imaging principally reflection data. Figure 8 has a low spatial frequency appearance since only reflections are imaged. This approach is useful for velocity analysis as the imaging is computationally very fast and we can add more p_s aperture as the velocity model becomes better determined.

Figure 9 increases the p_s aperture to -0.6 to +0.6 sec/km about each plane wave being imaged and the result shows improved spatial resolution as more diffracted energy is included in the final image.

Conclusions

We have shown that modern seismic data can be transformed into source, receiver, or offset plane wave components and these compact data can be imaged to depth with minimal (i.e. source and receiver position independent) travel time computations. Staging over plane wave aperture is a useful tool for velocity analysis as we can concentrate on reflected arrivals and form trial images rapidly. High spatial resolution imaging can be performed by simply adding more source plane wave components as the velocity model becomes better known, which is particularly advantageous for 3D applications. Finally, the methods described here can be implemented for anisotropy by simply changing the vertical delay time algorithm and appropriate amplitude corrections.

References

Fokkema, J.T. and P.M. van den Berg, 1993, *Seismic applications of acoustic reciprocity*, Elsevier Science Publishers B.V.

Hildebrand, S.T., and Carrol, R.J., 1993, Radon depth migration: Geophysical Prospecting, Vol. 41, p229-240.

Mukherjee, A., Sen M.K., Stoffa P.L., 2005, Traveltime computation and pre-stack time migration in transversely isotropic media, J. Seismic Exploration (submitted for publication).

Levander, A.R., 1988, Forth-order finite-difference *P-SV* seismograms: Geophysics, Vol. 53, p1425-1436.

Schneider, W.A., 1978, Integral formulation for migration in two and three dimensions: Geophysics, Vol. 43, p49-76.

Schneider, W.A., Jr., Ranzinger , K.A., Balch, A.H., and Kruse, C., 1992, A dynamic programming approach to first arrival traveltime computation in media with arbitrarily distributed velocities: Geophysics, Vol. 57, p39-50.

Schultz, P.S., Claerbout, J.F., 1978, Velocity estimation and downward continuation by wavefront synthesis: Geophysics, Vol. 43, 691-714.

Stoffa, P.L., Buhl, P., Diebold, J.B., and Friedemann, W., 1981, Direct mapping of seismic data to the domain of intercept time and ray parameter – A plane wave decomposition: Geophysics, Vol. 46, p255-267.

Stolt, R.H., 1978, Migration by Fourier transform: Geophysics, Vol. 43, p23-48.

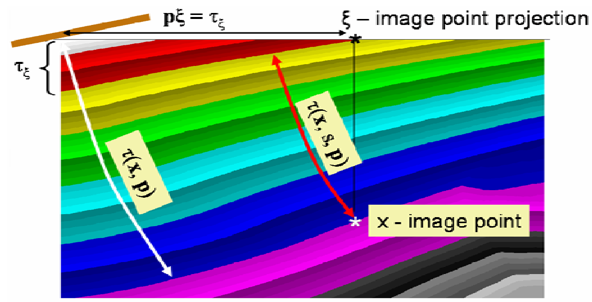

Figure 1. Isochrons and plane wave vertical delay times

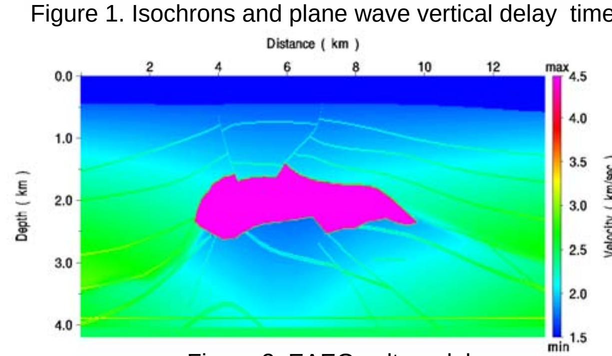

Figure 2. EAEG salt model

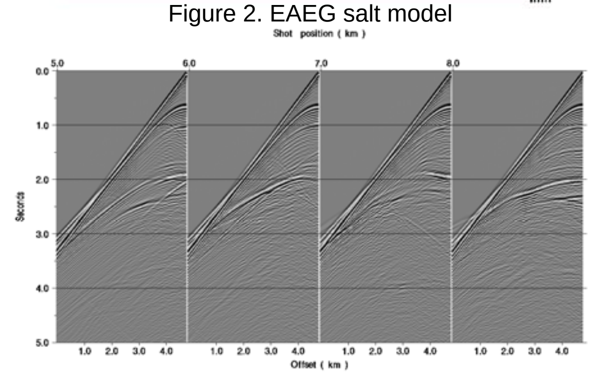

Figure 3. Finite difference common shot gathers at source positions 5, 6, 7 and 8 km simulating a marine survey with the array towed behind the ship. 240 channels were acquired with a receiver spacing 20m. The maximum offset is 4.78 km

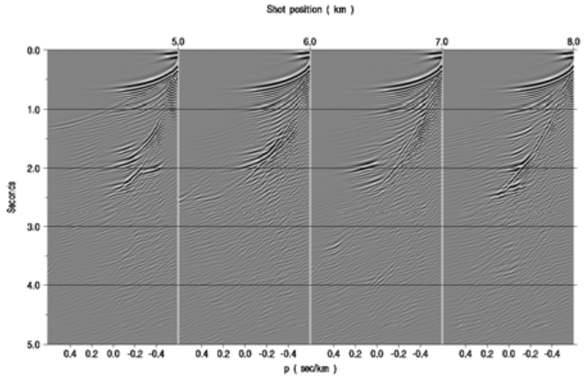

Figure 4. $\tau - p$ transformed shot point gathers at source positions 5, 6, 7 and 8 km. 121 traces in each panel correspond to ray parameters from +0.6 to -0.6 sec/km every 0.01 sec/km

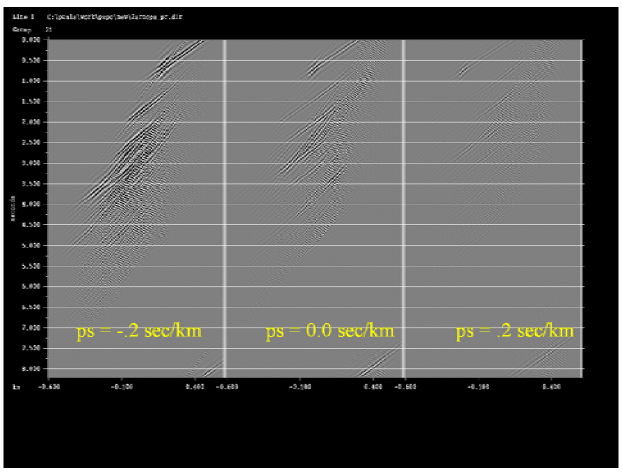

Figure 5. p_s cross sections from $p_s - p_r$ volume

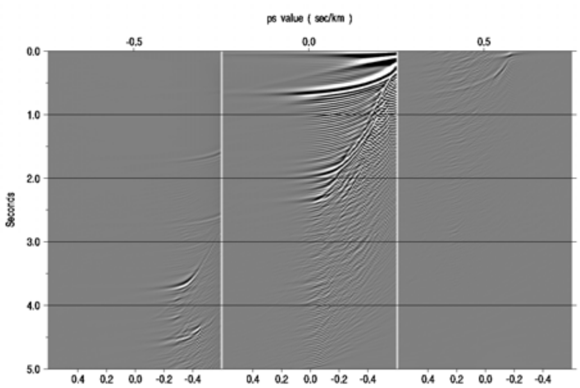

Figure 6. p_s cross sections from $p_s - p_o$ volume

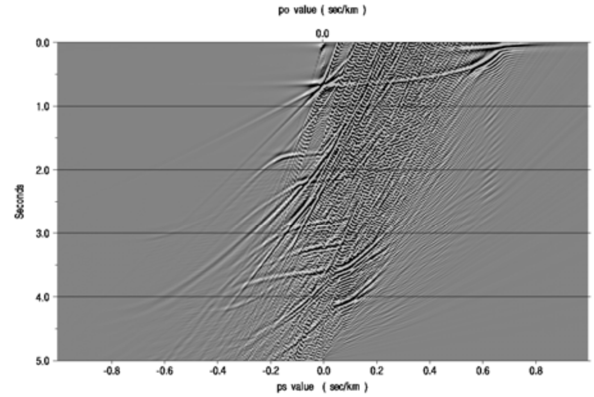

Figure 7. p_o =0.0 cross section from $p_s - p_o$ volume

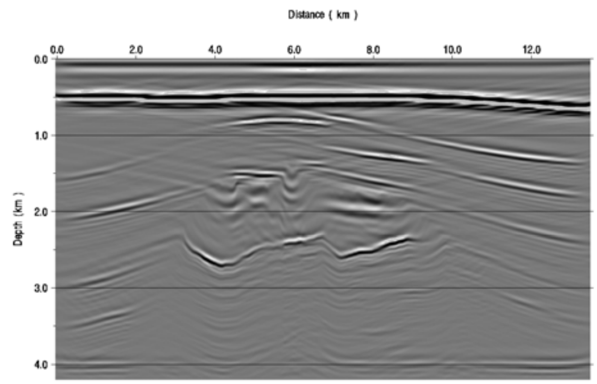

Figure 8. $p_s - p_o$ migrated shot gather: p_s values range from -0.1 to 0.1 sec/km, p_o values range from -0.6 to 0.6 sec/km

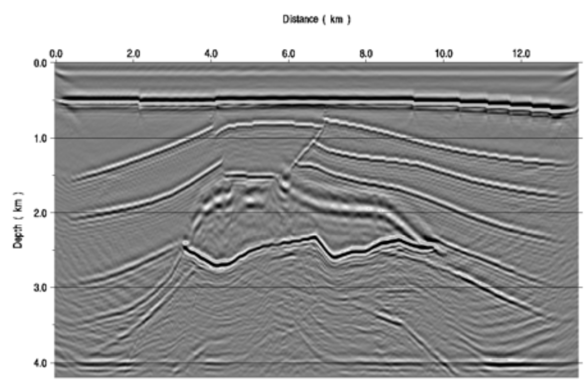

Fiigure 9. $p_s - p_o$ migrated shot gather: p_s values range from -0.6 to 0.6 sec/km, p_o values range from -0.6 to 0.6 sec/km